Available online at www.sciencedirect.com

ScienceDirect

Procedia CIRP 107 (2022) 295–301

www.elsevier.com/locate/procedia

55th CIRP Conference on Manufacturing Systems

In-line Sensor-based Process Control of the Calendering Process for Lithium-Ion Batteries

Andreas Mayr[a, *], David Schreiner[a], Benedikt Stumper[a], and Rüdiger Daub[a]

[a]*Institute for Machine Tools and Industrial Management, Technical University of Munich, Boltzmannstr. 15, 85748 Garching, Germany*

* Corresponding author. Tel.: +49-89-289-16584; fax: +49-89-289-15555. *E-mail address:* andreas.mayr@iwb.tum.de

Abstract

The calendering process is the final property-defining step in the manufacturing of electrodes for lithium-ion batteries. Calendering significantly affects mechanical properties by compacting the electrodes and increases the lithium-ion batteries' volumetric energy density. The choice of calendering parameters is primarily based on empirical data, considering the final battery cell properties. The drive for increased energy densities and the corresponding high compaction rates results in an increased electrode defect and scrap occurrence. This leads to challenges in process control which are addressed in this paper by developing an agile and predictive sensor-based process control. Hereby an efficient determination of process parameters is enabled, resulting in a reduction of scrap and manufacturing costs. Applying in-line data acquisition for electrode thickness and surface topography allows real-time feedback of measurement data at the machine-product interface back into the calendering system control. Reliable data acquisition is established by integrating two sensor systems for coating thickness measurement (confocal sensors) and defect detection (laser triangulation sensor) in a cascaded arrangement, enabling real-time evaluation of the product properties achieved as a function of the process parameters. The associated potentials and challenges regarding a predictive analysis of machine and product behavior are addressed in this context. The experimental results demonstrate that the combination of both sensor systems offers the potential to establish an agile and innovative process control for the calendering process of lithium-ion batteries.

Keywords: lithium-ion battery, electrode production, calendering, sensor integration, process control

1. Introduction

More than 80 % of the energy consumed worldwide is generated from fossil fuels [1], which are one of the main contributors to greenhouse gas emissions and thus lead to global warming [2]. Lithium-ion battery (LIB) technology enables off-grid storage of renewable energy in addition to representing a central component for the successful transition from fossil fuel-powered vehicles to electric-powered means of transportation. The application of high-performance and cost-efficient LIBs in the automotive sector reduces CO_2 and NO_x emissions [3]. The resulting growing demand for LIBs (with high requirements for energy and power density [3, 4]) results in challenges regarding the manufacturing processes in battery production.

The manufacturing process of LIBs consists of highly interlinked production steps, divided into electrode manufacturing and cell assembly [5]. To achieve a high market penetration of electric vehicles, a decrease in manufacturing costs – primarily dominated by high rejection rates due to scrap – is essential [6, 7]. An in-depth analysis and optimization of individual electrode manufacturing processes, in addition to the materials used, is one of the main levers for improving the electrochemical properties of LIBs, e.g., energy density, and reducing manufacturing costs [3].

2212-8271
10.1016/j.procir.2022.04.048

Electrodes of LIBs consist of a composite of active material particles, binders, and conductive additives coated as a suspension on a metal foil serving as the current collector. Evaporation of the solvent within the electrode suspension used in the coating process leads to a porous microstructure at the end of the electrode drying process [8]. Calendering, the final property-defining production step in electrode manufacturing, significantly affects the mechanical and electrochemical properties of the electrodes. During calendering, the electrodes of the LIBs are compacted between two rolls, thus reducing the pore volume within the coating and increasing the volumetric energy density of the LIBs [9, 10]. The drive for increased energy densities and the corresponding requirement for high compaction rates results in an increased occurrence of electrode defects and scrap [6]. Due to substantial material costs [11], the rejection rate resulting from scrap and calendering-induced electrode defects significantly affects the quality-cost correlation of the produced electrodes. The required reduction in rejection rates leads to challenges in process control which are addressed in this paper by developing an agile and predictive process control based on surface topography.

2. State-of-the-Art: Calendering Process

Electrochemical and mechanical properties of the calendered electrodes depend on the electrode properties obtained from preliminary processes and the choice of calendering parameters [12]. After drying, the electrodes possess a high initial porosity and are then compressed in the calendering process to a lower porosity to increase the volumetric energy density [9, 10]. The target porosity is determined considering the trade-off between high ionic conductivity (high porosity and low compaction rate) and high electrical conductivity (low porosity and high compaction rate) [13, 14]. The porosity reduction is equivalent to an increase in electrode density and a decrease in electrode thickness.

The compaction of electrodes is associated with the homogenization of the mechanical electrode properties [15], resulting in a lower deviation of the product quality in terms of observed cycle performance and discharge capacity of the LIBs [16]. Furthermore, the targeted adjustment of the porosity leads to an increase in cohesion within the coating (particle-to-particle contact) [14] and affects the process time and the behavior in the subsequent wetting process [17].

The morphology of the active material used for the LIBs significantly influences the calendering behavior and affects the development of defect patterns [9]. Only few studies describe the defect patterns induced during the calendering of electrodes [6, 18, 19]. Günther et al. [6] classified calendering-induced defect patterns into geometric, structural, and mechanical defects and evaluated the influence of their occurrence on subsequent process steps. Mayer et al. [19] investigated the effects of the mechanical behavior of electrodes after compaction on the electrochemical cell performance and the singulation into sheets.

An increased roll temperature can partly compensate for the appearance of defect patterns due to reduced line load and thus mechanical stresses applied throughout the process [3, 6, 9]. Raising the roll temperature enables a reduction in the necessary line load [12] and the achievable porosity [20–22], as well as an increase in adhesion strength [20, 23].

Modeling (analytical [4, 20] and simulation-based [24–28]) of the calendering process is increasingly used as an addition to experimental analysis and opens up new opportunities to determine properties and target parameters in advance. Schreiner et al. [27] developed a discrete element method (DEM) model to support the selection of suitable process parameters to reduce the adjustment effort for calendering and manufacturing costs simultaneously.

Machine parameters of the respective calendering system play a decisive role in calendering behavior. Depending on the calendering system used, different machine behavior, e.g., characteristic roll displacement curves during compaction, can be observed [12]. Larger roll diameters lead to an elevated adhesion strength of the calendered electrodes [12, 23] and simultaneously increase the intervention zone between rolls and electrode, thus reducing the shear forces exerted on the electrode during calendering [3, 23].

To the best of our knowledge, the calendering process and its agile control based on the required target properties and product characteristics are only scarcely considered in the state-of-the-art. Overall, no adequate process monitoring exists in pilot production lines for LIBs, characterized by missing sensor data and low data quality [29]. In this paper, two sensor systems for defect detection and coating thickness measurement are integrated into the calendering system at the Institute for Machine Tools and Industrial Management (*iwb)* at the Technical University of Munich (TUM) to enable in-line data acquisition of the product properties as a function of the process parameters. With an agile and predictive process control based on surface topography, the objective is to build up a more profound process knowledge regarding the parameter selection for calendering and reduce manufacturing costs of LIBs at production ramp-up by reducing scrap due to defect patterns.

3. Experimental

The experimental overview provides a description of the calendering system used and the investigated electrodes. Furthermore, the integrated measurement systems and data processing methods are addressed.

Calendering system: In the pilot production line for LIBs at the *iwb*, the EA 102 model from Coatema Coating Machinery GmbH is used. The same machine was used for preceding studies on electrode defects [6] and calendering behavior [9, 12]. The calendering system has two rolls with a width and diameter of 400 mm both, and ensures a maximum line load of 1000 $N \cdot mm^{-1}$ along an operating width of 300 mm. The maximum achievable roll temperature is 150 °C. The web speed range covers 0.1–3 $m \cdot min^{-1}$. The experiments for the presented paper were performed with a web speed of 0.5 $m \cdot min^{-1}$.

Measurement systems: The correlation of process parameters with quantifiable product properties was established by integrating two sensor systems for coating thickness measurement (confocal sensors) and defect detection

(laser triangulation sensor) in a cascaded arrangement. The focus of the sensor system for defect detection was on the two defect patterns electrode corrugation and corrugations at the coating edge, which have proven to be dominant defects based on experience and previous studies [6, 9]. The laser triangulation sensor (LJ-V7200, Keyence, Germany) [30] was integrated directly after the roll gap, enabling quantification and evaluation of electrode defects in the form of three-dimensional (3D) height profiles and two-dimensional (2D) corrugation measurements.

Sensors for confocal coating thickness measurement (CL-L030, Keyence, Germany) [31] were positioned after the roll gap and in front of the first deflection roller following a support roller. The latter was subsequently integrated after preliminary testing to improve the web guidance between the confocal sensor heads and increase the measuring accuracy. All measurements for coating thickness and defect detection were conducted with frequencies of 1000 Hz and 500 Hz, respectively. To evaluate the accuracy of the confocal coating thickness measurement, the electrodes were additionally measured manually with a tactile dial gauge (ID-C112AX, Mitutoyo, Germany). Fig. 1 shows an overview of the calendering system at the *iwb* and the integrated in-line measurement systems.

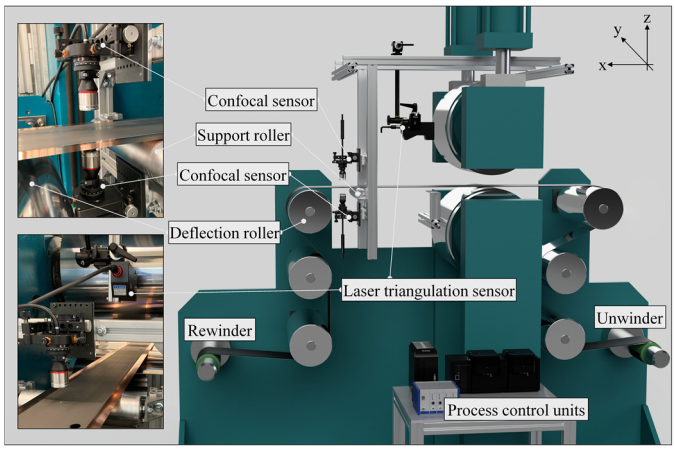

Fig. 1. Overview of the measurement systems and their integration in the calendering system at the *iwb*.

Data processing: Data processing and analysis was conducted on a Windows workstation after the data had previously been processed in the associated process control units. The internal control software of the confocal sensors calculated the specific coating thickness out of the distance values of the sensor heads relative to the electrode web. The coating thickness was measured with a moving average of 1024 data points. The goal was to evaluate the suitability of the confocal measurement system for applications within a closed-loop control system. For individual sections of the analyzed electrode, the confocal mean value was compared to the mean value of the tactile coating thickness measurement in terms of consistency.

Processing of the laser triangulation measurement data consisted primarily of two steps: (1) smoothing of the raw signal by applying a Savitzky-Golay filter [32], a low-pass filter which used a window with a length of 300 data points for smoothing, and (2) detrending, whereby the polynomial trend of the smoothed measurement signal was removed. In the latter step, the objective was to highlight the intensity of the detected defect patterns, i.e., their amplitude span as an oscillation around the zero-crossing. For comparative analysis among electrodes and to determine the process capability, the defect evaluation index (DEI) is introduced within the scope of this work. The value for DEI was calculated from the difference in magnitude between the lowest valley and the highest peak of the detected corrugation signal of the defective electrode. Continuous evaluation of the electrode profile and assessment of the defect patterns for defined electrode areas using DEI aims at facilitating process stability and agile control of the calendering process. The profile line of the laser triangulation sensor allows monitoring of half of the electrode width, which is 150 mm. As the defect patterns studied in the experimental part of this paper are formed approximately symmetrically, this does not affect the evaluation of the defect patterns of interest.

Electrode materials and composition: Cathodes with lithium- and manganese-rich nickel-cobalt-manganese oxide (LMR-NCM) active material have proven susceptible to defect patterns in previous experimental studies [9] and were therefore used for the analysis of defect patterns in this paper. The composition of the LMR-NCM cathodes is similar to that presented by Schreiner et al. [9], i.e., 92.5 wt% LMR-NCM ($Li_{1.14}[Ni_{0.26}Co_{0.14}Mn_{0.60}]_{0.86}O_2$ investigated by Teufl et al. [33], BASF, Germany), 4 wt% conductive carbon black (SuperC65, Imerys, Switzerland) and 3.5 wt% polyvinylidene-fluoride binder (PVdF) (Solef 5130, Solvay, Belgium) with an uncalendered dry electrode thickness of ≈ 150 µm (corresponds to ≈ 56 % porosity).

Proof of applicability and functionality of the coating thickness measurement was evaluated on graphite anodes, composed of 94 wt% graphite (SMG-A5, Showa Denko, Germany), 3 wt% styrene-butadiene rubber (SBR) (BM-451B, Zeon, Germany), 2 wt% carboxymethyl cellulose (CMC) (MAC500LC, Inabata, Germany) and 1 wt% conductive carbon black (SuperC65, Imerys, Switzerland) with an uncalendered dry electrode thickness of ≈ 215 µm (corresponds to ≈ 55 % porosity). Due to the available equipment setup and the resulting defect patterns, preliminary tests have shown that coating thickness measurement is only feasible for uncalendered and slightly calendered cathodes. The high precision requirement of the in-line sensor technology leads to a narrow precision measuring range of ± 1.0 mm in z-direction (point measurement, light spot diameter: 500 µm), which is exceeded when corrugations are present. Cathodes and anodes were coated on both sides on 15 µm thick aluminum foil (Type 1050 A, Korff, Switzerland) and 10 µm thick copper foil (Cu-PHC, SE-Cu58, Schlenk, Germany), respectively.

4. Results and Discussion

4.1. In-line Data Acquisition

Studies by Schreiner et al. [9] demonstrated that LMR-NCM cathodes exhibit significant defect patterns at the investigated porosities of 42 % and 32 %, making further processing of the electrodes challenging [6]. This was attributed to the low

elastic deformability of LMR-NCM cathodes and was associated with an additional internal porosity within the secondary LMR-NCM agglomerates [9]. The integrated in-line sensor technology uses laser triangulation to quantify these defect patterns in a continuous roll-to-roll process. Fig. 2 shows the 3D height profile of an LMR-NCM cathode with a coating thickness of ≈ 100 µm (corresponding to a porosity of ≈ 30 %) with a schematic illustration of the measuring area. The dashed lines in Fig. 2 correspond to the measurement location for the defect patterns: a) corrugations at the coating edge and b) electrode corrugation. The 3D electrode surface is color-coded according to the height scale (limit range between ± 5 mm). Values outside the limit range are displayed according to the color-coding with the respective maximum color value.

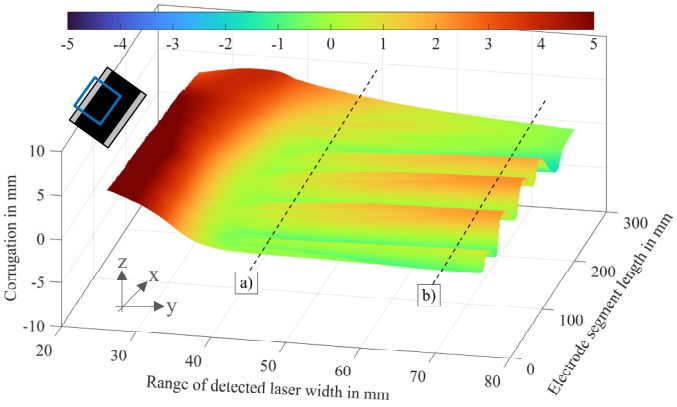

Fig. 2. 3D height profile of an LMR-NCM cathode with ≈ 30 % porosity (calendered at ambient temperature of ≈ 23 °C) and the position of the analyzed measurement signals: a) corrugations at the coating edge, b) electrode corrugation.

Fig. 2 shows the visible formation of geometric defects induced by the calendering process in the form of significant corrugations. Accordingly, the electrode's corrugation intensity is reflected in a clear distinction between the valley and the peak of the defect patterns in terms of the corresponding color-coding. In the coating edge area (in the range of the detected laser profile at ≈ 35–45 mm), smaller corrugations are evident, which are superimposed with the electrode corrugation. The formation of the smaller corrugations is locally limited to the immediate coating edge area. The curvature of the substrate foil is influenced by the overall curvature of the electrode web. In the presented Fig. 2, a curvature of the substrate foil can be seen in the positive z-direction, up to the limit of the color-coded height scale at + 5 mm, i.e., the entire LMR-NCM cathode has a bowl-shaped curvature across the coating width.

The compaction of LMR-NCM cathodes, strongly affected by the defect patterns described by Schreiner et al. [9], can be confirmed and evaluated in the 3D height profile through laser triangulation. Considering the height scale, an evaluation of the intensity of the respective defect patterns is made possible. This is supplemented by calculating the DEI values for the measurement signals of the respective geometric defects (represented by the dashed lines in Fig. 2), and the intensity of the corrugations is quantified.

Fig. 3 shows the superposition of the measured signals of the electrode corrugation and the corrugations at the coating edge, respectively, for the LMR-NCM cathode with a porosity of ≈ 30 %, which correspond to the 3D height profile in Fig. 2. In addition, the range of peak-to-valley values and the calculated DEI values are visualized.

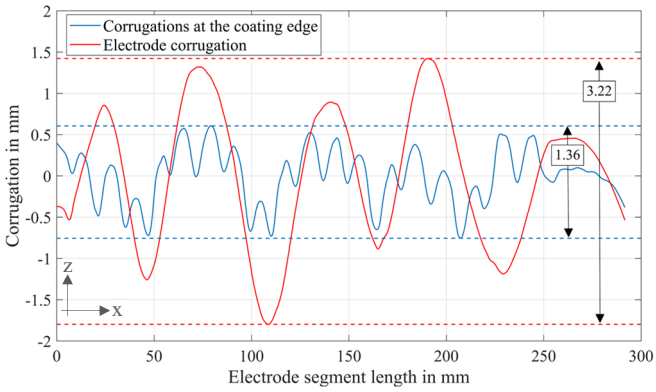

Fig. 3. Quantification of the defect patterns for the LMR-NCM cathode with ≈ 30 % porosity (calendered at ambient temperature of ≈ 23 °C) using the DEI as an evaluation metric.

Characteristics of the 3D height profile are reflected in the 2D representation of both measurement signals. The DEI value for the defect pattern of the electrode corrugation is quantified with 3.22. For the formation of corrugations at the coating edge, the DEI is lower, with a value of only 1.36. Superposition of the two curves is also evident, according to which electrode corrugation leads to an increase (or respectively decrease) in the position of the corrugations at the coating edge relative to the zero-crossing.

In accompanying experiments, the impact of the roll temperature (an increase from 23 °C to 90 °C) on the intensity of the defect patterns of LMR-NCM cathodes with a constant porosity level of ≈ 30 % was evaluated by means of DEI. The respective DEI values registered a reduction of 25.2 % for the electrode corrugation and 9.6 % for the corrugations at the coating edge. Prior to integrating the in-line sensor technology, defect patterns were only evaluated qualitatively. Quantification of the correlation between the intensity of geometric defects and the degree of calendering supports the introduction of a DEI as an evaluation metric regarding the formation of defect patterns.

The confocal coating thickness measurement was evaluated using graphite anodes with respect to its suitability for use in agile process control. As previously stated, exceeding the measuring range when calendering cathodes and the associated corrugations pose a challenge. In Fig. 4, the sensitivity of the confocal measurement system during calendering of graphite anodes is evaluated. Starting from the uncalendered section (1), the graphite anode was compacted with an applied calendering pressure of 100 % (2). The initially set roll gap was in the order of ≈ 140 µm. The change in coating thickness was achieved by reducing the calendering pressure to 85 % (3), 75 % (4), 50 % (5), and finally to 0 % (6) to return to the uncalendered state. The pressure reduction results in an increase in the effective roll gap. At the moment of the experimental measurements, it was impossible to quantify the resulting roll gap due to the lack of in-line gap measurement.

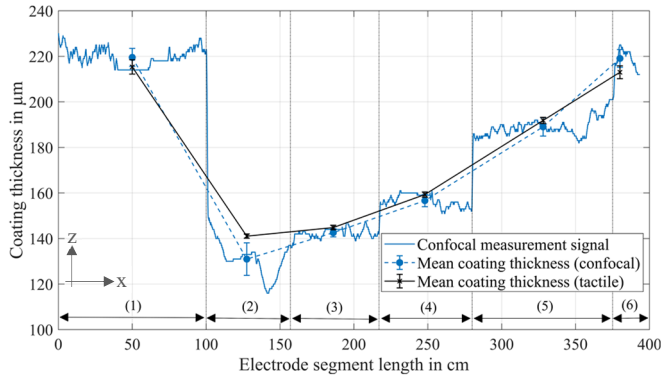

Fig. 4. Confocal coating thickness measurement of a graphite anode during calendering and comparison of tactile and confocal mean values.

Averaged over all electrode sections (1–6), a mean deviation of 4.7 µm is achieved between the confocal and tactile coating thickness measurements. In particular, the agreement reached between the confocal coating thickness measurement and the tactile measurement in electrode sections (3–5) should be highlighted, as the difference in the mean values is only in a range of 2.3–2.8 µm. One hypothesis for the increased deviation in electrode section (2) is the transition from the uncalendered to the calendered area, where the anode surface of the latter is associated with a gloss effect that affects the light reflected from the electrode surface and thus the accuracy of the optical measurement technique. It has been shown that compacted electrode surfaces, in contrast to uncalendered ones, have a pronounced gloss effect [34]. The confocal measurement system allows good repeatability and sufficiently accurate measurement of the coating thickness of graphite anodes (under the conditions that are optimizable in terms of integration in the present measurement setup).

Based on the presented results and conclusions, a topology for the implementation of an agile process control based on in-line sensor technology in the form of a cascaded arrangement was developed. Additionally, further practical measures and requirements for the optimized integration of the measuring systems into a calendering system were derived.

4.2. Conceptual Process Control

The schematic topology of a cascaded closed-loop control system is demonstrated in Fig. 5. The arrows inside the calender rolls indicate the direction of rotation.

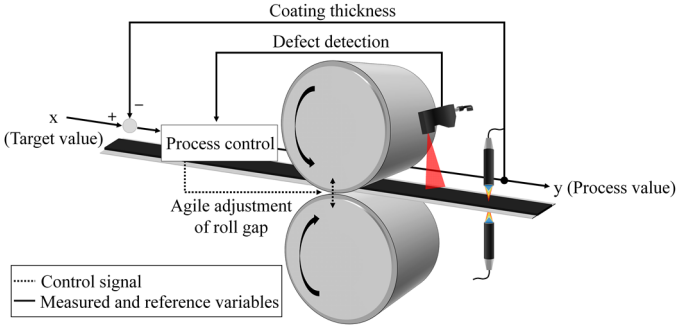

Fig. 5. Conceptual design of an agile process control in a closed-loop via defect detection and coating thickness measurement of the electrode web.

The laser triangulation sensor is cascaded upstream of the confocal coating thickness measurement as an indicator system. The quantification and comparability of defect patterns detected by laser triangulation are facilitated by applying the data processing and calculation of DEI values. Prior to the calendering process, a target value for the coating thickness is specified in an application software and compared with the confocally measured coating thickness (defined as *process value*). The roll gap is adjusted within an agile and closed feedback loop based on the deviation via the intelligent process control system. The latter refers to the implementation of data processing methods in the internal process control in the form of algorithms and artificial intelligence. Simultaneously, the electrode profile is monitored longitudinally and transversely to the direction of web movement concerning defect patterns. Based on this procedure, tolerance limits as well as lower and upper warning and intervention thresholds regarding DEI are defined. In application, a process warning is given as an indicator for the potential formation of defect patterns. Based on the warning and intervention thresholds, it is possible to automatically adjust the coating thickness in the closed-loop process control for optimized mechanical electrode properties and subsequent processing of the electrodes.

Accordingly, defect detection serves as a safeguarding system, based on which the accuracy of the confocal coating thickness measurement can be assessed. In the case of corresponding corrugations, an influence on the measurement accuracy with regard to the coating thickness of the electrode can be assumed. Coupling the two sensor systems leads to a broader understanding of the calendering process and agile process control. It simultaneously ensures lean quality assurance by correlating process parameters with product properties, for instance, the relationship between quantified defect patterns and the corresponding process parameters. The evaluation through DEI facilitates counteracting defect patterns by an agile adjustment of process parameters.

4.3. Requirements for Process Control via Thickness Measurement and Surface Topography

Regarding mechanical integration of the confocal measuring system, the vibration-decoupled mounting of the sensor heads, e.g., in the form of a traversing C-shaped mounting, is of particular importance. This also enables periodic calibration of the process control software during operation using an electrode sample with defined surface properties. Considering the varying optical properties of the electrode surface, this is an essential step for increasing the measurement accuracy. To reduce the effect of defect patterns on the confocal measurement signal, e.g., due to corrugations, especially during the compaction of cathodes, adapted web guidance and measurement position are necessary. This relates to introducing web tension isolation after the roll gap since an unevenly distributed web tension is eliminated, representing a disturbance variable. This allows the setting of a wide web tension window and can reduce corrugations. Concerning defect detection, several laser triangulation sensors are necessary to characterize the complete electrode web along the coating width regarding the classified defect patterns. In this

context, the use of sensors with different resolutions is intended to detect even minor electrode corrugations (e.g., the embossing of the substrate foil [6]).

5. Conclusion

As a property-determining process, calendering plays a crucial role in optimizing the cell's energy density and thus advancing LIB technology. A deeper process understanding via experimental studies and the subsequent development of a predictive and agile process control based on in-line sensor technology are addressed in this paper.

Applying in-line data acquisition for electrode thickness and surface topography allows real-time feedback of measurement data at the machine-product interface back into the calendering system control. First experimental results demonstrated that the combination of both sensor systems offers the potential to establish an agile and innovative control of the calendering process. A defect evaluation index (DEI) is introduced as a metric to evaluate defect detection via laser triangulation concerning defect patterns. The comparison of confocal with tactile coating thickness measurement for graphite anodes shows sufficient agreement between the two measurement methods for the present experimental setup. For the coating thickness measurement of cathodes, no sufficient results were achieved due to the difficulties associated with corrugations and the limiting measuring range of the confocal sensor technology. Based on the findings of the experimental study, further steps were derived for both measuring systems concerning the integration into an intelligent calendering system. This involves the planned integration of multiple laser triangulation sensors for a complete characterization of the electrode surface.

Future studies intend to investigate the relationship between compaction degree, roll temperature and intensity of defect patterns on different materials and compare the results for varying process parameters. The identification of defined tolerance limits based on capability indices as well as lower and upper warning and intervention thresholds for individual defect patterns and material systems will be implemented in future work. This will be carried out within the framework of extensive empirical studies based on the research conducted in this paper.

Acknowledgements

The authors gratefully acknowledge funding from the German Federal Ministry of Education and Research (BMBF) within the projects InteKal (grant number 03XP0348B), MiKal (grant number 03XP0240C), and ExZellTUM II (grant number 03XP0081). Many thanks to Michael Schüßler and Moritz Kupec for the support and fundamental work regarding sensor integration and data processing during experimental sessions. Special thanks to Fabian Konwitschny for the valuable discussion and proofreading of the manuscript.

References

[1] BP p.l.c., 2021. *bp Statistical Review of World Energy 2021*, London.
[2] Dincer, I., Colpan, C.O., Kadioglu, F., Editors, 2013. *Causes, Impacts and Solutions to Global Warming*. Springer New York.
[3] Kwade, A., Haselrieder, W., Leithoff, R., Modlinger, A. *et al.*, 2018. Current status and challenges for automotive battery production technologies *3*, p. 290.
[4] Meyer, C., Kosfeld, M., Haselrieder, W., Kwade, A., 2018. Process modeling of the electrode calendering of lithium-ion batteries regarding variation of cathode active materials and mass loadings *18*, p. 371.
[5] Günther, T., Billot, N., Schuster, J., Schnell, J. *et al.*, 2016. The Manufacturing of Electrodes: Key Process for the Future Success of Lithium-Ion Batteries *1140*, p. 304.
[6] Günther, T., Schreiner, D., Metkar, A., Meyer, C. *et al.*, 2020. Classification of Calendering-Induced Electrode Defects and Their Influence on Subsequent Processes of Lithium-Ion Battery Production *8*.
[7] Westermeier, M., Reinhart, G., Steber, M., 2014. Complexity Management for the Start-up in Lithium-ion Cell Production *20*, p. 13.
[8] Stein, M., Mistry, A., Mukherjee, P.P., 2017. Mechanistic Understanding of the Role of Evaporation in Electrode Processing *164*, A1616-A1627.
[9] Schreiner, D., Zünd, T., Günter, F.J., Kraft, L. *et al.*, 2021. Comparative Evaluation of LMR-NCM and NCA Cathode Active Materials in Multilayer Lithium-Ion Pouch Cells: Part I. Production, Electrode Characterization, and Formation *168*.
[10] Meyer, C., Bockholt, H., Haselrieder, W., Kwade, A., 2017. Characterization of the calendering process for compaction of electrodes for lithium-ion batteries *249*, p. 172.
[11] Nelson, P.A., Ahmed, S., Gallagher, K.G., Dees, D.W., 2019. *Modeling the Performance and Cost of Lithium-Ion Batteries for Electric-Drive Vehicles, Third Edition*.
[12] Schreiner, D., Oguntke, M., Günther, T., Reinhart, G., 2019. Modelling of the Calendering Process of NMC-622 Cathodes in Battery Production Analyzing Machine/Material-Process-Structure Correlations *7*.
[13] Gulbinska, M.K., Editor, 2014. *Lithium-ion Battery Materials and Engineering*. Springer London.
[14] Zheng, H., Tan, L., Liu, G., Song, X. *et al.*, 2012. Calendering effects on the physical and electrochemical properties of $Li[Ni_{1/3}Mn_{1/3}Co_{1/3}]O_2$ cathode *208*.
[15] Haselrieder, W., Ivanov, S., Christen, D.K., Bockholt, H. *et al.*, 2013. Impact of the Calendering Process on the Interfacial Structure and the Related Electrochemical Performance of Secondary Lithium-Ion Batteries *50*, p. 59.
[16] Lenze, G., Bockholt, H., Schilcher, C., Froböse, L. *et al.*, 2018. Impacts of Variations in Manufacturing Parameters on Performance of Lithium-Ion-Batteries *165*, A314-A322.
[17] Habedank, J.B., Günter, F.J., Billot, N., Gilles, R. *et al.*, 2019. Rapid electrolyte wetting of lithium-ion batteries containing laser structured electrodes: in situ visualization by neutron radiography *102*, p. 2769.
[18] Bold, B., Fleischer, J., 2018. Kalandrieren von Elektroden für Li-Ionen-Batterien *113*, p. 571.
[19] Mayer, D., Wurba, A.-K., Bold, B., Bernecker, J. *et al.*, 2021. Investigation of the Mechanical Behavior of Electrodes after Calendering and Its Influence on Singulation and Cell Performance *9*, p. 2009.
[20] Meyer, C., Weyhe, M., Haselrieder, W., Kwade, A., 2020. Heated Calendering of Cathodes for Lithium-Ion Batteries with Varied Carbon Black and Binder Contents *8*.
[21] Primo, E.N., Chouchane, M., Touzin, M., Vazquez, P. *et al.*, 2021. Understanding the calendering processability of $Li(Ni_{0.33}Mn_{0.33}Co_{0.33})O_2$-based cathodes *488*.
[22] Primo, E.N., Touzin, M., Franco, A.A., 2021. Calendering of $Li(Ni_{0.33}Mn_{0.33}Co_{0.33})O_2$-Based Cathodes: Analyzing the Link Between Process Parameters and Electrode Properties by Advanced Statistics *4*, p. 834.
[23] Billot, N., Günther, T., Schreiner, D., Stahl, R. *et al.*, 2020. Investigation of the Adhesion Strength along the Electrode Manufacturing Process for Improved Lithium-Ion Anodes *8*.
[24] Ngandjong, A.C., Lombardo, T., Primo, E.N., Chouchane, M. *et al.*, 2021. Investigating electrode calendering and its impact on electrochemical performance by means of a new discrete element method model: Towards a digital twin of Li-Ion battery manufacturing *485*.
[25] Sangrós Giménez, C., Schilde, C., Froböse, L., Ivanov, S. *et al.*, 2019. Mechanical, Electrical, and Ionic Behavior of Lithium-Ion Battery Electrodes via Discrete Element Method Simulations *8*.
[26] Duquesnoy, M., Lombardo, T., Chouchane, M., Primo, E.N. *et al.*, 2020. Data-driven assessment of electrode calendering process by combining experimental results, in silico mesostructures generation

and machine learning *480*.
[27] Schreiner, D., Klinger, A., Reinhart, G., 2020. Modeling of the Calendering Process for Lithium-Ion Batteries with DEM Simulation *93*, p. 149.
[28] Schreiner, D., Lindenblatt, J., Günter, F.J., Reinhart, G., 2021. DEM Simulations of the Calendering Process: Parameterization of the Electrode Material of Lithium-Ion Batteries *104*, p. 91.
[29] Wanner, J., Weeber, M., Birke, K.P., Sauer, A., 2019. Quality Modelling in Battery Cell Manufacturing Using Soft Sensoring and Sensor Fusion - A Review, in *2019 9th International Electric Drives Production Conference (EDPC)*, p. 1.
[30] Keyence DEUTSCHLAND GmbH. LJ-V7200. https://www.keyence.de/products/measure/laser-2d/lj-v/models/lj-v7200/. Accessed 20 November 2021.
[31] Keyence DEUTSCHLAND GmbH. CL-L030. https://www.keyence.de/products/measure/laser-1d/cl-3000/models/cl-l030/. Accessed 20 November 2021.
[32] Schafer, R., 2011. What Is a Savitzky-Golay Filter? [Lecture Notes] *28*, p. 111.
[33] Teufl, T., Strehle, B., Müller, P., Gasteiger, H.A. *et al.*, 2018. Oxygen Release and Surface Degradation of Li- and Mn-Rich Layered Oxides in Variation of the Li_2MnO_3 Content *165*, A2718-A2731.
[34] Meyer, C. *Prozessmodellierung der Kalandrierung von Lithium-Ionen-Batterie-Elektroden,* 1st edn.